Biophysical Journal Volume 105 September 2013 1432–1443

Membrane Partitioning of the Pore-Forming Domain of Colicin A. Role of the Hydrophobic Helical Hairpin

Ivan L. Bermejo,[†] Cristina Arnulphi,[‡] Alain Ibáñez de Opakua,[†] Marián Alonso-Mariño,[†] Félix M. Goñi,[†§] and Ana R. Viguera[†*]

[†]Unidad de Biofísica (CSIC, UPV/EHU), Barrio Sarriena s/n, Leioa, Spain; [‡]Facultad de Matemática, Astronomía y Física, Universidad Nacional de Córdoba, Córdoba, Argentina; and [§]Departamento de Bioquímica, Universidad del País Vasco, Leioa, Spain

ABSTRACT The colicins are bacteriocins that target *Escherichia coli* and kill bacterial cells through different mechanisms. Colicin A forms ion channels in the inner membranes of nonimmune bacteria. This activity resides exclusively in its C-terminal fragment (residues 387–592). The soluble free form of this domain is a 10 α-helix bundle. The hydrophobic helical hairpin, H8–H9, is buried inside the structure and shielded by eight amphipathic surface helices. The interaction of the C-terminal colicin A domain and several chimeric variants with lipidic vesicles was examined here by isothermal titration calorimetry. In the mutant constructions, natural sequences of the hydrophobic helices H8 and H9 were either removed or substituted by polyalanine or polyleucine. All the constructions fully associated with DOPG liposomes including the mutant that lacked helices H8 and H9, indicating that amphipathic rather than hydrophobic helices were the major determinants of the exothermic binding reactions. Alanine is not specially favored in the lipid-bound form; the chimeric construct with polyalanine produced lower enthalpy gain. On the other hand, the large negative heat capacities associated with partitioning, a characteristic feature of the hydrophobic effect, were found to be dependent on the sequence hydrophobicity of helices H8 and H9.

INTRODUCTION

Each of the three different domains of colicins appears to perform a different function: 1), the central regions form unique structures that bind to outer membrane receptors; 2), the N-termini act in unknown ways during the transport of the toxin through the outer membrane; and 3), the C-termini contain the toxic activities of colicins; e.g., formation of voltage-gated pores in the cytoplasmic membrane by colicin A (see (1,2) for reviews).

Plasmid-encoded colicin A from *Citrobacter freundii* inserts into and forms pores in target bacterial inner membranes. In vitro, its C-terminal domain (pf-ColA) interacts spontaneously in moderately acidic solutions with negatively charged lipidic vesicles (3,4). The crystal structure of the water-soluble state of pf-ColA was shown to consist of a bundle of 10 helices (5,6) (Fig. 1). Among these, helices H8 and H9 form a hairpin that constitutes the hydrophobic core of the protein. The membrane-bound conformation is not known in detail. Two models for the closed-channel state of colicins have been proposed, the umbrella (6) and penknife (7) models. The main difference between them is the relative orientation of the H8–H9 hydrophobic helical hairpin with respect to the plane of the membrane: perpendicular or nearly parallel, respectively. Experimental evidence for both modes of interaction of pf-ColA with bilayers have been obtained: i), studies by fluorescence energy transfer (7), partial proteolysis and mass spectrometry (8), and disulfide bond engineering (9) support the penknife model; whereas ii), electron paramagnetic resonance analyses are in favor of the umbrella conformation (10). Moreover, published results agree with a view for the closed form of the homolog pore-forming domain of colicin E1 that would be compatible with the umbrella model (11–13). It is conceivable that the membrane-bound structure consists of an ensemble of conformations whose distribution depends on external parameters such as pH, lipid composition, temperature, or others.

Isothermal titration calorimetry (ITC) allows direct measuring of the heat changes and associated thermodynamics for biomolecular processes in aqueous solution. Energetics of peptide and protein insertion into lipid bilayers has been the object of extensive studies (14–16). The major driving force for partitioning solutes into nonpolar phases is universally assumed to be the hydrophobic effect, arising from the tendency of nonpolar molecules to avoid contact with water. Partitioning into membranes, however, is more complicated than simple phase partitioning, in fact enthalpy is often dominant in membrane partitioning (14,17).

In this study, the sequence of helices H8 and H9 has been substituted by polyamino acidic sequences of alanine and leucine, or deleted, and interaction energies have been compared to those obtained for the wild-type (WT) domain using ITC. Those two helices are confined to the protein core in its soluble conformation and are proposed to insert into the hydrophobic matrix of the membrane in the closed channel according to the umbrella model. The results obtained for the various species, with different structural contents and hydrophobicities, provide information on the

Submitted April 30, 2013, and accepted for publication August 12, 2013.

*Correspondence: gbbviria@ehu.es

Alain Ibáñez de Opakua's present address is Structural Biology Unit, CIC bioGUNE, Parque Tecnológico de Bizkaia Ed. 800, 48160 Derio, Spain.

Editor: William Wimley.

0006-3495/13/09/1432/12 $2.00

http://dx.doi.org/10.1016/j.bpj.2013.08.012

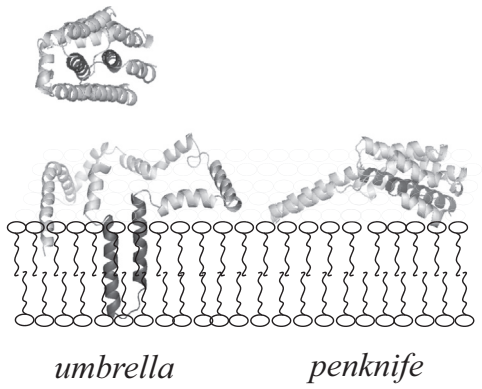

FIGURE 1 Ribbon representation of the soluble (1COL.pdb) and putative bound conformations of pf-ColA. Helices H8 and H9 are highlighted in black.

respective roles of hydrophobic and amphipathic helices in colicin A binding to membranes.

MATERIALS AND METHODS

Protein expression and purification

A 206-residue long construct corresponding to the colicin A residues 387 to 592 was cloned into the ampicillin-resistant plasmid pBAT4 and expressed in the *Escherichia coli* strain BL21(DE3). Cells were grown at 37°C to an OD 600 of 0.4–0.6 and induced with 1 mM IPTG (isopropyl α-D-thiogalactopyranoside). Four hours after induction the cells were harvested, resuspended, sonicated, and ultracentrifuged at 100,000 $\times$ *g*. The supernatant was subsequently purified on a HiLoad 26/60 Superdex 200 column (GE Healthcare) and a MonoQ HR 5/5 column (GE Healthcare). The deletion mutant mut-Ø mutant was obtained in a similar way. The soluble cellular fraction of mut-Ala and mut-Leu mutants were loaded to a 16/30 Phenyl-Sepharose (GE Healthcare) and eluted with Milli Q quality water. The fractions containing the protein were then concentrated and applied to a HiLoad 26/60 Superdex 200 column (GE Healthcare) for further purification and conserved at –80°C in 1 mg/ml aliquots. Average protein purification yields were around 40 (pf-ColA), 20 (mut-Ø), 10 (mut-Ala), and 3 (mut-Leu) mg per liter of culture, respectively. pf-ColA (22 kDa) and mut-Ø behaved as monomers at neutral and moderately acidic preparations as was shown by conventional size exclusion chromatography (SEC), whereas mut-Ala and mut-Leu showed different degrees of polymerization. Mut-Leu eluted in broad peaks with apparent mean molecular mass of 139 kDa. SEC was used in combination with a multiple-angle light scattering device to more precisely determine molecular mass of the polymers observed for mut-Ala. At neutral pH mut-Ala showed monomer/tetramer equilibrium, whereas only monomers were observed after incubating the samples at moderately acidic pH values. More details will be published elsewhere.

Liposome preparation

1,2-di-oleoyl-*sn*-glycero-3-phosphatidyl-glycerol (DOPG) was purchased from Avanti Polar Lipids (Birmingham, AL). For liposome preparation, DOPG was dissolved in chloroform/methanol (2:1, v/v), and the mixture was evaporated to dryness under a stream of nitrogen. Traces of solvent were removed by evacuating the samples under high vacuum for at least 2 h. The samples were hydrated at 45°C in the buffer obtained after protein dialysis, 50 mM sodium acetate pH 4.0 or pH 5.0, helping dispersion by stirring with a glass rod. The solution was frozen in liquid nitrogen and defrozen at 45°C 10 times. Large unilamellar vesicles (LUVs) were prepared by the extrusion method (18), using polycarbonate filters with a pore size of 0.1 μm (Nuclepore, Pleasanton, CA). Vesicle sizes were determined by dynamic light scattering using a Malvern Zetasizer instrument (Malvern, UK). The average vesicle diameter was 90–100 nm.

Circular dichroism (CD)

Far-UV (190–250 nm) CD spectra were recorded with a Jasco J-810 spectropolarimeter previously calibrated with d-10-camphorsulphonic acid. The device was equipped with a Jasco PTC-423S temperature controller and cuvettes were thermostated at 20°C. Protein concentration was 0.05 mg/ml in 50 mM sodium acetate buffer pH 5.0 in a 0.2 cm cuvette. Just before measurement, samples were centrifuged for 15 min at 14,000 $\times$ *g* in an Eppendorf microcentrifuge and 4°C. In the protein complexes with DOPG LUVs, lipid/protein ratios were always higher than 200; lower ratios gave rise to protein loss due to aggregation in the lipidic surface. The solvent spectrum was subtracted from the sample spectra, and data were converted to mean residue ellipticity.

Assuming that the mean residue ellipticity at 222 nm is exclusively due to the α-helix conformation, fractional helicities were calculated using the following equation

$$\%\ \text{helicity} = \frac{\left(-[\theta]_{222\ \text{nm}} + 2,340\right)}{30,300}, \qquad (1)$$

where $[\theta]_{222\ \text{nm}}$ is the observed mean residue ellipticity at 222 nm, and 2,340 deg cm^2 dmol^{-1} and 30,300 deg cm^2 dmol^{-1} are previously determined values corresponding to 0% and 100% helix content at 222 nm, respectively (19).

Thermally induced unfolding was monitored by CD at 222 nm in 0.2 cm pathlength cuvettes in the temperature range 10–90°C. The temperature was increased stepwise by 0.2°C at a rate of 60°C/h, and the ellipticity was recorded with a 1 nm bandwidth and a 2 s response. Melting temperatures (T_m) were calculated as the maxima of the first derivatives of the temperature transition curves.

ITC

The reaction enthalpy, ΔH, measurements were performed by ITC, with a VP-ITC microcalorimeter (MicroCal, Northampton, MA). Proteins were extensively dialyzed against buffer 50 mM sodium acetate pH 4.0 or 5.0, before titration. When the dialysis was complete external buffer was reserved for liposome preparation and subsequent dilutions. Both lipid and protein solutions were degassed under vacuum immediately before use. Successive injections (10 μL) of colicin (50 μM) were made via a rotating stirrer-syringe into the calorimetric cell containing 1.4283 mls of 1 mM DOPG large unilamellar liposomes. Injections were made at intervals of 10 to 20 min, and the duration of each injection was 2 s/μL of injected protein. To ensure proper mixing after each injection, a constant stirring speed of 300 rpm was maintained during the experiment. Experiments were performed with peptide/lipid molar ratios of 0.005/0.083 at constant temperature from 20 to 35°C. In control experiments, fresh protein solutions were titrated into pure buffer to obtain the dilution heat, which was negligible in all cases. Buffer into buffer and buffer into lipid suspension experiments were also conducted with identical minor heat changes, and were not taken into further consideration. The ionization enthalpy of the buffer, sodium acetate, is very low, 0.12 kcal mol^{-1} (20) and was also ignored.

RESULTS

Pf-ColA comprises the C-terminal residues 387–592 of the colicin A sequence. In what follows, the numbering will refer to amino acid position within this fragment (from 1 to 206 instead of 387 to 592 of the entire protein). Chimeric variants were created by a combination of the eight

amphipathic helices of pf-ColA with 38-residue long sequences of polyalanine and polyleucine. The tripeptide GPG was included in the middle of two stretches of 19 amino acids to facilitate flexibility between both helices. With mut-Ala and mut-Leu we will refer to the construction pf-ColA(1–148) $(aa)_{19}$ GPG $(aa)_{19}$ pf-ColA(190-206) where aa is alanine and leucine, respectively. The deletion mutant pf-ColA(1–148) GPG pf-ColA(190–206) was also analyzed (mut-Ø).

CD analysis

In the crystal structure of the pore-forming domain (6), 154 out of the 206 residues of pf-ColA (74%) are in α-helical conformation. CD spectra of the different polypeptides were recorded in 50 mM sodium acetate at pH 5.0 (Fig. 2). Table 1 summarizes the molar ellipticities at 222 nm of the native domain and mutants, and the corresponding α-helical contents according to Eq. 1 (Experimental procedures section). Calculated helical fraction of the WT domain correlates reasonably with the crystal structure. The drastic mutations exercised on pf-ColA have slight effects on the domain helical content. Only the mut-Ø mutant is substantially less helical (10–14%) than the WT domain. The thermal denaturation transition recorded for the different constructions at 222 nm in the 10–90°C range shows that high cooperativity is observed only for pf-ColA, whereas both cooperativity and melting temperature decrease for the mutants. The shallow transition is centered at 52°C for mut-Ø and mut-Ala and at 66°C for mut-Leu, whereas WT pf-ColA looses 50% of the helical content in a single sharp transition at 72°C (Fig. 2 *B*). This indicates that the mutants, although with very high helical contents, are not properly folded. This behavior resembles what has been observed for pf-ColA in acidic solutions and been described as a molten globule (4). These forms contain high levels of secondary structure in the absence of helix packing (21,22). The acidic molten globule of pf-ColA has been proposed as the membrane interacting intermediate (4). Thus, the absence of tertiary interactions in the mutants could circumvent some unfolding limiting steps in the insertion reaction.

Incorporation of pf-ColA to LUVs made of DOPG causes an increase of the negative CD signal at 222 nm (Fig. 2 *C*), which has also been observed for the homologous pf-ColE1 (13). The increment in helical content upon interaction is around 10% for pf-ColA. All mutants, even mut-Ø, reach similar values of $\theta_{222\ nm}$ in the lipid-bound conformation (Table 1). The higher helical content in the lipid-bound forms of proteins is compatible with either i), real helix extension induced by the nonpolar character of the membranous environment that promotes hydrogen bonding in certain protein loops or ii), the entropic repulsion or decrease in the number of accessible configurations available to a polymer chain in the bilayer with lower helical fluctuations (23,24). Apart from the increase in the negative signal at 222 nm, the spectral change induced by DOPG also includes an increase in the positive signal at 193 nm. A mere increase in helical content would also imply a parallel increment in the negative signal at 208 nm. However, $\theta_{208\ nm}$ hardly varies. As a consequence, the $\theta_{222\ nm}/\theta_{208\ nm}$ ratio changes from 0.96 ± 0.03 for the free proteins to 1.12 ± 0.03 in the lipid-bound domains. Similar spectral distortions have been illustrated in the transition from helix to coiled-coils (25–29) and also frequently in proteins embedded in bilayers (30–32), including pf-ColA (33) and pf-ColE1 (13). It has been proposed that the parallel polarized amide π-π^* transition becomes less dichroic, effectively reducing

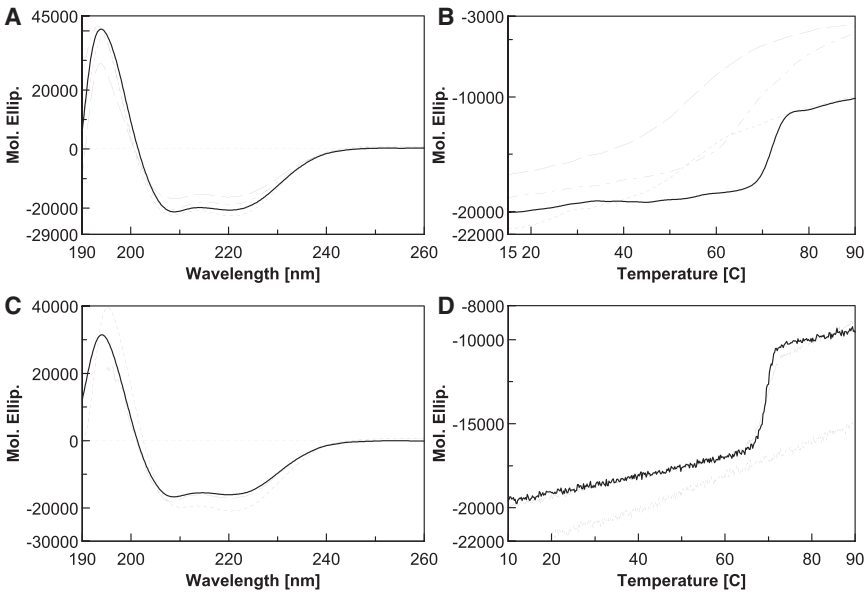

FIGURE 2 CD spectra (*A*) and temperature scans (*B*) recorded for the soluble conformations of WT pf-ColA (*continuous*), mut-Ø (*dashed*), mut-Ala (*dotted*), and mut-Leu mutants (*dash-dotted*) in 50 mM sodium acetate pH 5.0. CD spectra (*C*) and temperature scans (*D*) of pf-ColA in the absence of lipid (*continuous*) and with DOPG (*dotted*), and DOPC (*dashed*) LUVs in 50 mM sodium acetate at pH 5.0. Protein concentration was 2.5 μM and lipid concentration was 1.3 mM. Wavelength scans were recorded at 20°C in a 2 mm cuvette. For temperature scans, the signal were recorded at 222 nm with a heating rate of 1°C/min. Molar ellipticity is expressed in deg cm^2 $dmol^{-1}$ units.

TABLE 1 Circular dichroism

	Soluble			Lipid bound	
	θ_{222}	% helix	T_m	θ_{222}	% helix
	deg cm^2 dmol^{-1}			deg cm^2 dmol^{-1}	
pf-ColA	20446	74%	72°C	23120	84%
mut-Ø	15964	60%	52°C	20068	74%
mut-Ala	19968	73%	52°C	20401	76%
mut-Leu	18482	70%	66°C	23321	85%

Molar ellipticity at 222 nm and helical content of pf-ColA and its variants measured for the free soluble forms and in the presence of DOPG LUVs. The midpoint of thermal transition T_m is indicated only for the free soluble proteins. Protein concentration was 2.5 μM and lipid concentration was 0 or 1.3 mM, respectively, in 50 mM sodium acetate pH 5.0 and 20°C.

the negativity of $\theta_{208\ nm}$ (34). Because $\theta_{222\ nm}$ is unaffected, it still represents a reliable measurement of helical conformation, whereas the $\theta_{222\ nm}/\theta_{208\ nm}$ ratio increases to values higher than 1. These deviations in the CD spectra have been attributed to optical artifacts arising from the particulate nature of the membrane suspensions (32) or because of bunching of the absorbing chromophores into a small space, leading to local concentrations far in excess of the average protein concentration in the solution (30,31). It is worth mentioning that the CD spectrum of pf-ColA in complex with OLPG (lyso-oleoyl-*sn*-Glycero-3-phosphatidyl-glycerol) micelles, where the protein resides as a monomer, shows a 6% higher ellipticity with identical spectral shape as the soluble form (data not shown). Furthermore, the far CD spectrum recorded in the presence of neutral 1,2-dioleoyl-*sn*-glycero -3-phosphocholine (DOPC) LUVs, is similar to the one recorded in the absence of lipids (Fig. 2 *C*), further suggesting that the proposed increase in helical content inside the membrane is not due to light scattering artifacts.

At variance with temperature scans recorded for the polypeptides in buffer, or in a mixture with DOPC LUVs, the $\theta_{222\ nm}$ signal of the complexes with DOPG LUVs changed only slightly and linearly in the 20°–90°C temperature range (Fig. 2 *D*), and the initial signal was completely recovered after cooling (data not shown). This implies that the secondary structure content of the membrane-bound protein is unaffected by heating to 90°C. This remarkable stability of the α-helical conformation in the membrane environment cannot be straightforwardly interpreted as typical of a well-folded compact structure containing long-range contacts. The lower dielectric constant of the membrane matrix favors H-bonds in the α-helical conformation, reducing the coordinate space available to membrane-bound proteins. Whereas the reference structure for energy calculations in soluble proteins is the random coil, this conformation is highly unstable and improbable within lipid bilayers. Unfolding events of membrane proteins would not be visualized as a α-helix/coil transition, because the helical conformation is, by far, the most stable conformation in apolar environments even in the absence of tertiary contacts (35–37). Nonetheless, the insensitivity to temperature of the helical content can be considered a characteristic feature of lipid-bound proteins. In the presence of DOPG LUVs, the chimeric variants: mut-Ø, mut-Ala, and mut-Leu showed the same small and linear temperature dependence of the $\theta_{222\ nm}$ signal in the 20–90°C range as the one shown in Fig. 2 *D* for WT pf-ColA, which corroborates their incorporation into the liposomes.

ITC

ITC measures directly the energy associated with a physical and/or chemical reaction triggered by the mixing of two components. The technique is ideal to measure the heat associated to interactions between biological molecules (38,39). In ITC experiments, the calorimeter cell (1.4283 ml) was filled with the suspension of lipid vesicles (100 nm diameter) and injections of 50 μM protein sample (10 μl) were made every 600 to 800 s in sodium acetate 50 mM (Fig. 3). Integration of the power peaks yields the heat of reaction, q_i, and normalization to the number of moles of protein bound per injection, n_i, leads to the molar heat of the reaction, which, at constant pressure, corresponds to the reaction enthalpy ΔH (40,41)

$$\Delta H = \frac{q_i}{n_i}. \quad (2)$$

In Fig. 4 the heat of reaction (measured by peak integration) as a function of the protein/DOPG molar ratio is represented.

Under these conditions, concentration of lipid greatly exceeds that of protein during the whole titration experiments, and all of the protein is completely bound to the membrane surface. Indeed, a higher concentration of reactant would provide more informative binding isotherms in a simple chemical binding reaction, where saturation of binding sites is expected. However, with the polypeptides under study the choice of concentrations for the ITC experiments was limited by protein aggregation upon the lipid surface occurring at [lipid]/[protein] ratios lower than ~200. Apart from particular examples of proteins that bind specifically to lipids at 1:1 or similarly low molar ratios, in general interactions between proteins and membranes cannot be envisioned as the products of simple binding chemical reactions, giving rise to complexes with a well-defined stoichiometry and specific geometry. The membrane more generally behaves as an additional phase immiscible with water, and provides a vast number of binding sites.

When a solute *S* is in the presence of two nonmiscible phases (e.g., aqueous and lipidic phases), it distributes between the two according to its affinity for each medium. This affinity can be quantified in terms of a partition coefficient, K_P

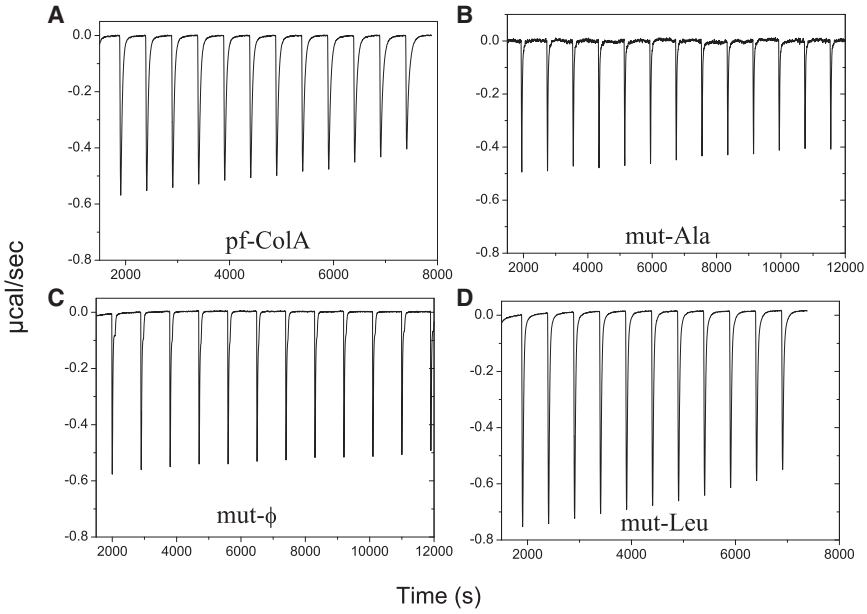

FIGURE 3 Calorimetric heat flows resulting from multiple injections of 10 microL aliquots of 50 mM pf-ColA (*A*), mut-Ala (*B*), mut-Ø (*C*), and mut-Leu (*D*) to a 1.4283 mL reservoir containing 1 mM DOPG LUVs in 50 mM sodium acetate pH 4.0 at 25°C.

$$K_p = \frac{[S_m]/V_m}{[S_w]/V_w} \approx \frac{[S_m]}{[S_w][L]V_\phi}, \tag{3}$$

where the subscripts w and m stand for aqueous and membrane-bound species respectively, V_m and V_w for lipid and aqueous solution volumes, $[L]$ to lipid concentration and V_ϕ to the lipid molar volume. The resulting expression is equivalent to the equation applicable for classical binding where binding sites are in great excess (42)

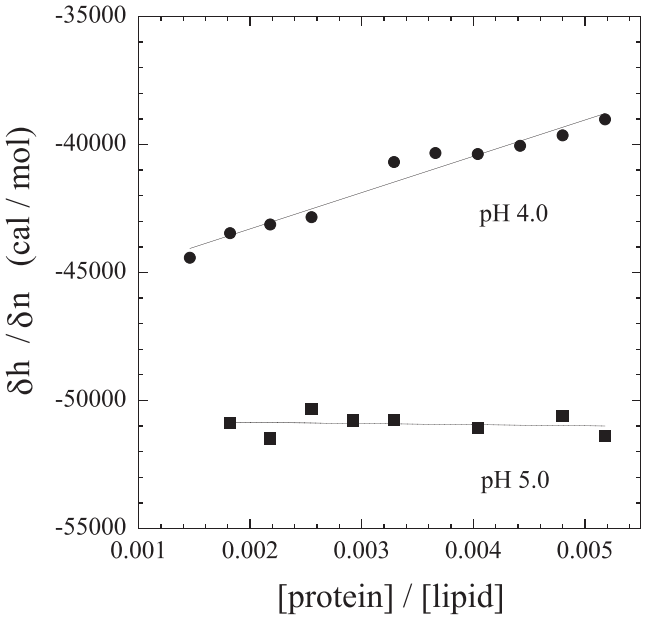

FIGURE 4 Heats of reaction obtained by peak integration, δh_i, normalized with respect to the injected number of moles, δn_i, obtained for titrations of DOPG LUVs with pf-ColA in 50 mM sodium acetate pH 4.0 (*circles*) and pH 5.0 (*squares*) at 20°C.

$$[S_m] = K_p[S_w][L]V_\phi. \tag{4}$$

Under the experimental conditions used here—very high partition coefficient and excess lipid—all added protein binds to lipid. Thus, in 50 mM sodium acetate pH 5.0, each injection of pf-ColA to DOPG LUVs produces almost the same exothermic heat effect. When the same experiment is performed by the addition of pf-ColA to neutral DOPC LUVs, heat production is negligible (not shown), further confirming the lack of interaction of pf-ColA with neutral lipids. DOPG vesicles are characterized by a negative surface potential leading to an attraction of the protein from bulk solution to the membrane surface. In contrast, the membrane potential of electrically neutral DOPC membranes is zero. Identical negative results were obtained in control buffer-into-lipid, protein-into-buffer dilution experiments.

Effect of pH on the interaction of pf-ColA with DOPG

WT pf-ColA, with an isoelectric point pI = 6.0, does not interact with lipid vesicles at neutral or basic pH values. At moderately acidic pHs, pf-ColA only incorporates into vesicles made of negative lipids. Charge excess in both, protein and lipidic surface, seems to be an essential condition for initial adsorption of the polypeptide onto the lipidic surface. Electrostatic attraction between the positively charged protein and the negatively charged lipid vesicles thus determines the onset of the complete insertion process.

The effect of pH on the interaction of pf-ColA with DOPG vesicles was studied by comparing ITC experiments performed at pH 4.0 and pH 5.0. At pH 5.0 the net protein charge is +3.59, whereas at pH 4.0 it is +12.74 (43).

Representative ITC profiles and the corresponding ΔH for measurements performed at pH 4.0 are shown in Figs. 3 and 4, and the thermodynamic parameters obtained are listed in Table 2. Measurements could be performed only within the narrow pH range of 4–5 because the protein does not interact with lipids above pH 5.0 and pHs lower than 4.0 drastically destabilize the protein. The midpoint of pf-ColA thermal denaturation T_m varies from 72°C to 70.2°C upon lowering the pH from 5.0 to 4.0 (data not shown).

At pH 4.0 the heat of reaction decreases gradually as the membrane properties change with more and more protein bound. Integration of the heat flow peaks in Fig. 3 yields reaction heats linearly dependent on the [protein]/[lipid] ratio (Fig. 4). Binding of protein molecules to the membrane can modify its properties and each new addition of free protein encounters a slightly different phase. It has been shown that electrostatic effects (44) or membrane saturation (45) could produce deviations from the partition model. The fact that the deviations of pf-ColA binding are pH-dependent and much larger when highly charged (at pH 5.0 each protein addition produces the same heat) indicates that they have an electrostatic basis. Bound protein decreases linearly the net charge of the bilayer due to charge compensation. Moreover, sterical hindrance or membrane shielding imposed by bound protein would not produce the observed linear relationship with the [protein]/[lipid] ratio.

The association enthalpy for pf-ColA/DOPG is ~7% higher at pH 4 than at pH 5.0 at 25°C (Table 2). On one hand, this increment can be explained by a higher electrostatic contribution to the interaction enthalpy at pH 4.0. On the other hand, an additional enthalpic cost is expected for protein unfolding at pH 5.0.

The role of hydrophobic helices H8–H9

In an attempt to dissect the contribution of the different protein regions to the overall enthalpy of binding, several chimeric mutants have been analyzed. Eight out of the 10 α-helices of pf-ColA are amphipathic. According to the proposed models for the closed channel of pf-ColA, these helices orient parallel to the membrane plane. These eight α-helices are common to all protein variants analyzed. The two hydrophobic α-helices H8 and H9 have been deleted in mut-Ø mutant and substituted by $(Ala)_{19}$-GPG-$(Ala)_{19}$ and $(Leu)_{19}$-GPG-$(Leu)_{19}$ in mut-Ala and mut-Leu mutants, respectively. Typical trace isotherms, enthalpy of reaction, and temperature dependence of the mutants are represented in Figs. 3, 5, and 6.

Mut-Ø versus pf-ColA

The most hydrophobic region, 38 out of the 206 residues (18.4%), of pf-ColA is missing in mut-Ø. The deletion mutant mut-Ø most conceivably interacts mainly with the membrane surface and interface, because insertion of any of the amphipathic helices in the bilayer hydrophobic core would be rather unfavorable in the absence of protein polymerization or induced transmembrane potential. Interaction enthalpies obtained for mut-Ø are, on average, only 17% less negative than those obtained for WT pf-ColA, at pH 4.0 and 5.0. The reaction enthalpy per residue is thus very similar. This suggests that hydrophobic helices are not major contributors to the binding enthalpy of pf-ColA. It should be considered however that mut-Ø, in contrast to WT, is not a properly folded protein.

In terms of secondary structure there are no major changes upon lipid binding in pf-ColA, whereas they are detectable in mut-Ø. It has been shown that helix formation at the membrane surface is a favorable process, $\Delta G_{helix} = -0.14$ kcal/mol residue, enthalpically driven, $\Delta H_{helix} \approx -0.7$ kcal /mol residue (46,47). This trend would benefit mut-Ø more than pf-ColA. Nevertheless, the main conformational differences between pf-ColA and mut-Ø are related to the native tertiary contacts that are absent in mut-Ø. Free pf-ColA native structure is destabilized on the lipidic negative surface in such a way that interhelical links are disrupted, thus allowing disarticulation of independent helices. Some positive side chains replace their intramolecular counterions by those of the lipid head group. Additionally, WT helices H8 and H9, absent in mut-Ø, move from the apolar interior of the protein to the similarly apolar interior of the bilayer. It is difficult to estimate the enthalpic contribution of these interchanges, but it is likely that the advantage at the level of secondary and tertiary structure of mut-Ø compensate to some extent the loss of interactions established by WT helices H8–H9 with the lipid.

TABLE 2 ITC

	pH	ΔH (20°C) (kcal/mol)	ΔH (25°C) (kcal/mol)	ΔH (30°C) (kcal/mol)	ΔH (35°C) (kcal/mol)	ΔC_p (kcal/mol.K)
pf-ColA	4.0	−44.6 ± 0.6	−55.4 ± 0.5	−60.7 ± 0.4	−67.8 ± 0.7	−1.5 ± 0.06
pf-ColA	5.0	−51.5 ± 0.6	−51.9 ± 0.5	−51.3 ± 0.4	−48.2 ± 0.9	−0.2 ± 0.08
Mut-Ø	4.0	−33.6 ± 0.2	−43.6 ± 0.4	−51.6 ± 0.6	−56.4 ± 0.9	−1.53 ± 0.07
Mut-Ø	5.0	−38.8 ± 0.3	−44.0 ± 0.2	−41.3 ± 0.2	−43.4 ± 0.6	−0.2 ± 0.07
Mut-Ala	4.0	−27.8 ± 0.5	−33.8 ± 0.5	−45.6 ± 0.6	−49.3 ± 0.5	−1.53 ± 0.07
Mut-Ala	5.0	−30.1 ± 0.5	−36.8 ± 0.6	−36.0 ± 0.8	−37.1 ± 0.7	−0.4 ± 0.1
Mut-Leu	4.0	−46.3 ± 0.6	−56.8 ± 0.2	−72.1 ± 0.2	−84.8 ± 0.6	−2.6 ± 0.05

Thermodynamic parameters calculated at [lipid]/[protein] = 1000, for pf-ColA (WT and derivatives) binding to DOPG LUVs in sodium acetate 50 mM.

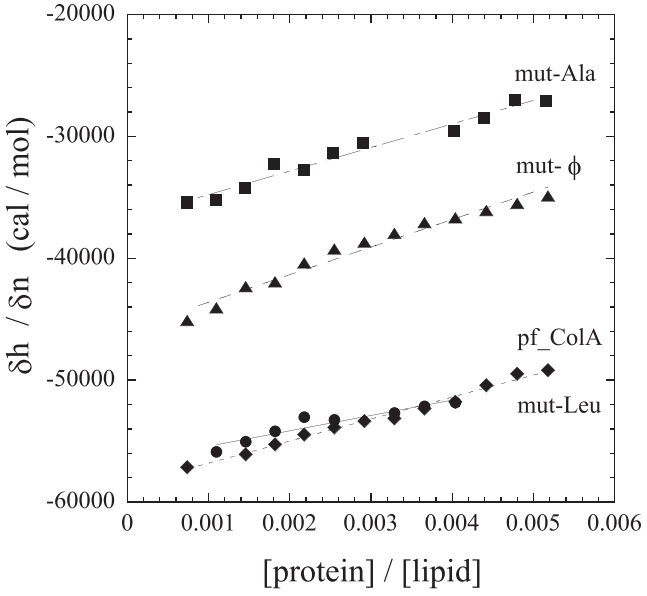

FIGURE 5 Heats of reaction of titrations of DOPG LUVs with mut-Ø (*triangles*), mut-Ala (*squares*), pf-ColA (*circles*) and mut-Leu (*diamonds*) in 50 mM sodium acetate pH 4.0 at 25°C.

Mut-Ø versus mut-Ala

The transfer energies of alanine from water to octanol and from water to membrane interface are +2.1 and +0.7 kJ/mol, respectively (37), suggesting poor partition in hydrophobic environments, however some experiments on helix propensities of polyalanine-based peptides in the presence of membranes seem to confirm that alanine slightly exceeds the hydrophobic threshold for membrane insertion (48). A 20 mer of polylalanine can be inserted into the bilayer with a free energy of ~ –5.5 kcal/mol (49). Furthermore, calculations (50) and experiments (49,51) have indicated that polyalanine stretches form stable complexes with bilayers. However, when polyalanine sequences were added in aqueous buffer to preformed vesicles, membrane insertion occurred with varying efficiency depending on length, solvent, concentration, and other parameters that influence the ensemble of conformations that the peptides can adopt, including aggregation and kinetically trapped configurations that reduce peptide insertion (49,52).

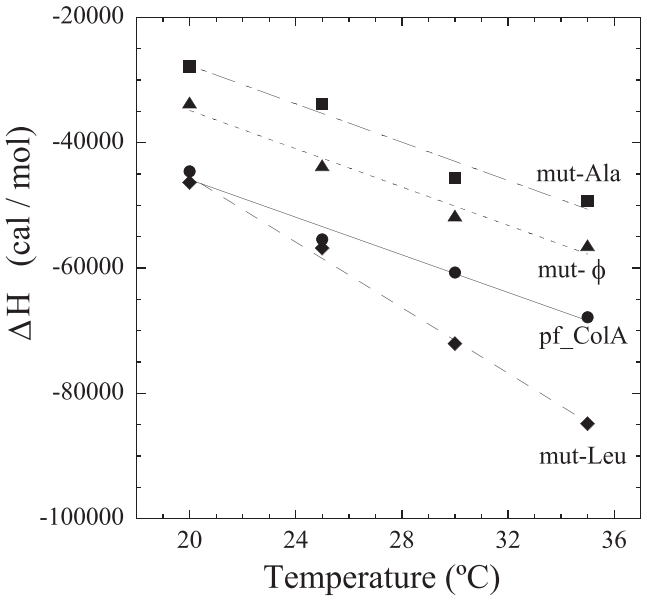

FIGURE 6 Temperature dependence of reaction enthalpies calculated at [lipid]/[protein] = 1000 of mut-Ø (*triangles*), mut-Ala (*squares*), pf-ColA (*circles*) and mut-Leu (*diamonds*) with DOPG LUVs in 50 mM sodium acetate pH 4.0.

The midpoint of the smooth transition observed at $\theta_{222\ nm}$ with temperature is 52°C for the free forms of both mutants, mut-Ø and mut-Ala. Thus, in the energetic comparison of mut-Ø and mut-Ala interaction with bilayers, conformational changes should not be playing a major role. Mut-Ala contains two additional arrays of 19 alanine residues with respect to mut-Ø. The additional 38 residues of mut-Ala did not represent an enthalpic gain in our experimental system. On average, 7 ± 2 kcal mol^{-1} were lost in the enthalpy changes induced by mut-Ala, as compared to mut-Ø, when added to DOPG vesicles. This result suggests that some negative (exothermic) enthalpy is lost or some positive (endothermic) contribution is gained in the interaction of mut-Ala with DOPG bilayers. Theoretically, our scaffold is compatible with either orientation, in-plane, or transmembrane, of polyalanine helices. Ala_{19} stretches are long enough to span the membrane, if transmembrane orientation were favored. In peptide-lipid codissolved mixtures, the transmembrane orientation was shown to account for 70–80% in 1-palmitoyl-2-oleoyl-*sn*-glycero-3-phosphocholine (POPC) bilayers for a K_3-A_{18}-K_3 sequence, which corresponds to a small average ΔG per-residue of ~ −0.2 kJ mol^{-1} for the in-plane/transmembrane orientation equilibrium (52). The membrane surface charge density, thus the membrane surface potential ψ is much larger in DOPG than POPC vesicles and it is predictable that the moderately apolar alanine is expelled from the surface to the interior of the bilayer, although myriad conformations and relative orientations are still possible. In either scenario, the enthalpy loss should be either compensated by some entropic advantage to justify the reported negative Gibbs free energy (49) or sustained by the rest of the polypeptide, in the absence of entropy gain, suggesting that the DOPG-bound conformation of polyalanine is disfavored with respect to free polyalanine.

Mut-Ala versus mut-Leu

In the mut-Leu chimera 38 leucine residues substitute the natural sequences of helices H8 and H9. In 50 mM sodium acetate pH 4.0 and 25°C, interaction enthalpies are −56.8 ± 0.2 and −33.8 ± 0.5 kcal mol^{-1} for mut-Leu and mut-Ala, respectively, which corresponds to 61 cal mol^{-1} for each Leu-to-Ala mutation. Replacing an alanine

by leucine increases the transfer energy from water to octanol by ~5–7.5 kJ mol^{-1} (1.2 –1.8 kcal mol^{-1}) (37) and transmembrane orientation is undisputed for polyleucine peptides (53).

Dilution control experiments of mut-Leu into buffer are not accompanied by any measurable heat exchange, and the mutant is soluble to high concentrations. However, size exclusion chromatography experiments showed that mut-Leu forms oligomers in aqueous solution and becomes monomeric in OLPG micelles (data not shown). The small calculated enthalpic change upon leucine to alanine mutation could be due to the different oligomeric states of both mutants in aqueous solution.

Temperature dependence. Heat capacity

All the reaction enthalpies observed upon titration of fluid DOPG vesicles with pf-ColA and its mutants decrease (higher negative values) with increasing temperature. The temperature dependence of ΔH is given by

$$\frac{\partial \Delta H}{\partial T} = \Delta C_p, \quad (5)$$

where ΔC_p is the heat capacity change at constant pressure during the reaction. The ΔC_p values derived from measurements performed in the 20 to 35°C range, are summarized in Table 2.

A semiempirical relationship of ΔC_p with changes in the accessible surface polar (ΔASA_{pol}) and apolar (ΔASA_{ap}) areas upon complex formation has been proposed (54):

$$\Delta C_p = 0.45\ \Delta ASA_{ap} - 0.26\ \Delta ASA_{pol}\ \text{cal mol}^{-1}\ \text{K}^{-1}, \quad (6)$$

ΔC_p values obtained at pH 4.0 are significantly lower than those at pH 5.0 (Table 2, Fig. 4) for WT, mut-Ala, and mut-Ø. None of the ionizable groups of pf-ColA are located in helices H8 and H9. Thus, there are no charge differences between the mutants and WT pf-ColA. All species gain around nine positive charges upon going from pH 5.0 to pH 4.0. Unexpectedly, ΔC_p is more negative in mixtures at pH 4.0, where electrostatic interactions should be more important. Usually ΔC_p is indicative of a release of water from hydrophobic surfaces (55). Although ΔC_p is also influenced by the release of water from the hydration shell in the interaction zone upon ion binding, this effect would produce a positive ΔC_p and thus counterbalance the effect that arises from hydrophobic dehydration. This implies that hydrophobic interactions between reactants take place or that the hydrophobic contacts between the membrane lipids are increased. In this respect, it was shown that the electrostatic binding of oligoarginine to heparin sulfate (a polyanion) produces a positive ΔC_p (56), whereas its binding to negatively charged DPPG membranes shows a negative ΔC_p, suggesting burial of arginine side-chain hydrophobic moieties within the membrane (57). Additionally, lipidic headgroup charge neutralization can have as a consequence a better packing of acyl chains of the lipid (57), justifying in part the observed more negative ΔC_p at pH 4.0.

Among the different mutants, the lowest ΔC_p is obtained for the mut-Leu chimera (−2.6 kcal mol^{-1} K^{-1}), whereas pf-ColA, mut-Ala, and mut-Ø have very similar values of ΔC_p (−1.5 kcal mol^{-1} K^{-1} Fig. 6, Table 2). If free and bound forms were conformationally identical in all the constructions assayed, ΔC_p would be roughly proportional to the hydrophobicity of the sequence of H8 and H9, provided that the umbrella model was truly representative of the bound form. The mean hydrophobicity of region H8–H9 is 1.8 in mut-Ala, 2.1 in pf-ColA, and 3.8 in mut-Leu (58). The higher value of $\Delta C_p = -1.5$ kcal mol^{-1} K^{-1} seems to be independent of the H8–H9 region and arises from partial penetration of amphipathic helices H1–H7 and H10 or from lipid-lipid contacts. The small difference in hydrophobicity of mut-Ala and pf-ColA may be insufficient to translate into a remarkable change in ΔC_p. More importantly, in the free form of pf-ColA, helices H8 and H9 are shielded from the bulk solvent by the rest of the structure and the difference in solvent exposure of H8–H9 may be small upon interaction with lipid. This compensation is not possible in mut-Ala, for which the structure of the free form does not seem to be unique and stable. The same reasoning is also valid for mut-Leu, however the considerably higher hydrophobicity of H8–H9 helices in this mutant is enough to cause a significant increase in ΔC_p, wholly compatible with a transmembrane orientation of polyleucine sequences, in accordance with previous results (53).

DISCUSSION

A full knowledge of membrane protein structure and folding requires an understanding of the energetics of protein insertion into and stability within lipid bilayers. ITC is a technique for monitoring binding and the method of choice for characterizing biomolecular interactions. When two components are bound, heat is either released or absorbed. Measurement of this heat allows to accurately determine binding constants, K_b, reaction stoichiometry, n, enthalpy, ΔH, and entropy, ΔS (59). However, the practical range of measurable binding constants by ITC is limited to ~10^3–10^8 M^{-1} (59). The enthalpy of binding of pf-ColA, mut-Ø, mut-Ala, and mut-Leu to lipid bilayers of DOPG were measured under conditions of a large excess of lipid, where self association of the proteins at the membrane surface was negligible and binding was dominated by peptide partitioning into the bilayer. The high affinity for DOPG bilayers guarantees that, under the experimental conditions used, all the protein injected binds to the membrane. Thus, a reliable binding constant or partition coefficient cannot be extracted and only the reaction enthalpy, ΔH,

can be determined with high precision from a given titration curve.

The complete process of the interaction of pf-ColA with bilayers can be envisioned as a series of sequential, coupled reactions. Each individual step has its own associated enthalpy, entropy, and Gibbs energy changes. The observed overall enthalpy would be a collection of all the individual contributions:

(i) Electrostatic attraction seems to be essential and sufficient for the in vitro association of pf-ColA with bilayers. The mutant mut-Ø, which lacks the most hydrophobic region of the protein, interacts with membranes with an enthalpy gain only 20–30% lower than that of the WT protein (Table 2), suggesting that the eight amphipathic helices H1–H7 and H10 are importantly contributing to the interaction with negatively charged lipids. The major driving force for partitioning solutes into nonpolar phases is universally assumed to be the hydrophobic effect, which arises from the tendency of nonpolar molecules to avoid contact with water. This makes the hydrocarbon core of lipid bilayers a favorable environment for nonpolar solutes (55). However, the apolar region of the membrane is protected from bulk solvent by the polar head group layer that represents an exceptional barrier for a hydrophobic polypeptide. Folding of constitutive membrane proteins is assisted by efficient insertion machineries that can surpass these barriers. On the contrary, interaction of amphitropic proteins (those that interconvert between aqueous and lipidic environments) with membranes should necessarily contemplate an unavoidable early acquaintance with the lipidic polar surface. Many amphitropic proteins use lipid clamp motifs designed for binding a unique lipid monomer (60,61), but a certain set of proteins bind to membrane through amphipathic helices (62,63). For the latter, nonpermanent binding can be conveniently modulated by ionic strength, anionic lipid content, suggesting that electrostatic attraction contributes to the binding, although the hydrophobic character of the amphipathic helix is also a key determinant of the binding strength (64).

(ii) Protein unfolding within the membrane surface has been shown to be rate-limiting in the interaction of pf-ColA with model membranes (3). Local pH decreased by ~1.5 units with respect to bulk pH at the surface of vesicles made of negative lipids (4). Neutralization of acidic residues would occur when pf-ColA is incorporated into the surface of DOPG vesicles (e.g., 24 out of the 27 acidic residues of the protein are protonated at pH 3.0). This would cause a disruption of most of the interhelical salt bridges and a dissociation of helices, thus highly destabilizing the tertiary structure. Such a conformational transition can also be observed at acidic pH in solution, in the absence of membranes (4). Unattached basic residues would instead ion-pair easily with lipidic negative headgroups. The energetic balance of this ion interchange is difficult to determine, although more electrostatic contacts are probably gained within the versatile highly charged lipidic surface than those that are lost within the native structure. Only the WT pf-ColA possesses a stable, unique native conformation. Compared to its mutants, with the same enthalpic gain pf-ColA would have an energetic extra penalty of unfolding. This would explain, in part, why pf-ColA does not show a more negative ΔH. Additionally and differently from many lipid-binding protein motifs, that become α-helical in the bound form but are random coils in solution (65–67), pf-ColA secondary structure does not change greatly upon binding. The interaction of pf-ColA to a bilayer membrane is not coupled with a random coil/α-helix transition, as frequently seen (Fig. 2).

(iii) It is expected that hydrophobic partitioning contributions can be deduced from the comparison of species that only differ in the hydrophobic region of helices H8 and H9 of pf-ColA. Mut-Ala contains two stretches of 19 alanines that, in principle, could locate parallel or perpendicular to the membrane plane. Previous data have shown that alanine peptides are at equilibrium between both orientations in POPC bilayers (52). It is also known that alanines are not specially favored at the surface of negatively charged vesicles (68). It appears that the energy gaps between the different locations, free, in-plane associated, and transmembrane bound is very small. Here, we show that DOPG-bound mut-Ala gains less enthalpy than mut-Ø (Table 2), suggesting that the productive interaction of the eight amphipathic helices of the protein sustains the otherwise enthalpically unfavorable polyalanine-lipid contacts. In the in-plain orientation, polyalanine probably displaces counterions and hydration shell water molecules, and in the transmembrane orientation it perturbs the efficient packing of lipid chains, with a loss in van der Waals energy in either case. Although the exact position of the hydrophobic helical hairpin in the membrane-bound state of WT pf-ColA has been a subject of controversy (6,7), the hydrophobicity of the residues in helices H8 and H9 is sufficient to penetrate within the hydrophobic interior of the membrane. The enthalpy gain with respect to mut-Ø is however relatively small, $<30\%$. As stated previously, at variance with its chimeric mutants, the inserted form of pf-ColA competes with a compact fully folded soluble free form in which protein groups are enjoying specific interactions. Thus, the energetic balance of pf-ColA contemplates more stable products and reactants than mut-Ø in the binding reaction. Conversely, leucine is one of the most hydrophobic amino acids and efficient hydrophobic partition

of polyleucine sequences into membranes is well documented (52,53). The enthalpy gain goes from moderate at room temperature to considerable (>30%) at 35°C with respect to pf-ColA, compatible with a transmembrane orientation of H8—H9 in both polypeptides.

Large negative standard heat capacity changes ($\Delta Cp << 0$) are the hallmark of processes that remove nonpolar surface from water, including the transfer of nonpolar solutes from water to a nonaqueous phase. The change of ΔH for mut-Leu binding to DOPG LUVs as a function of temperature yields a ΔCp of -2.6 kcal mol^{-1} K^{-1}, suggesting burial of the nonpolar surface area and is consistent with the penetration of the hydrophobic hairpin into the bilayer (69). pf-ColA containing the less hydrophobic natural hairpin H8–H9, however, does not render a ΔCp value significantly higher than mut-Ø, -1.5 kcal mol^{-1} K^{-1}, in which this protein region is missing. This indicates that the shielding from bulk water of the hydrophobic hairpin is as efficient in the folded free protein as in the interior of the bilayer in the bound form, producing as a result no net change in ΔCp.

CONCLUSION

Partitioning into bilayers is much more complicated than bulk-phase partitioning, because the anisotropic and heterogeneous nature of bilayers (15,16) and serious difficulties are encountered when attempting to distinguish the separate contributions to interaction thermodynamics in such complex systems. The observed values result from intricate balances of multiple effects of different sign. Here, we have tried to deconvolute some of the enthalpic contributions of pf-ColA interaction with negative lipids by the use of chimeric variants with polyamino acidic sequences. As a summary, the binding of pf-ColA and its mutants to negative DOPG in the fluid phase is exothermic and therefore energetically favored. Because of the difficulties in obtaining reliable values for the binding constants, it remains unclear whether there is also an increase in entropic contribution to the free energy of binding. The interactions established by the eight amphipathic helices H1 to H7 and H10 contribute significantly to the enthalpy of binding, to a degree that is sufficient for full protein association with vesicles, even when fused to sequences with moderate affinity for lipids such as polyalanine. Additionally, electrostatic binding of the positively charged pf-ColA to the negatively charged DOPG bilayer contributes to protein-lipid binding. Further enthalpy gain directly depends on the hydrophobicity of helices H8–H9, higher negative values being obtained for more hydrophobic sequences.

I. Bermejo and A. Ibáñez de Opakua are indebted to the Departamento de Educación, Universidades e Investigación (GobiernoVasco), Consejo Superior de Investigaciones Científicas (I3P) and Fundación Biofísica Bizkaia for predoctoral fellowships.

This work was funded by grant BFU2006-14423/BMC (MEC).

REFERENCES

1. Cao, Z., and P. E. Klebba. 2002. Mechanisms of colicin binding and transport through outer membrane porins. *Biochimie.* 84:399–412.
2. Cascales, E., S. K. Buchanan, …, D. Cavard. 2007. Colicin biology. *Microbiol. Mol. Biol. Rev.* 71:158–229.
3. González-Mañas, J. M., J. H. Lakey, and F. Pattus. 1992. Brominated phospholipids as a tool for monitoring the membrane insertion of colicin A. *Biochemistry.* 31:7294–7300.
4. van der Goot, F. G., J. M. González-Mañas, …, F. Pattus. 1991. A 'molten-globule' membrane-insertion intermediate of the pore-forming domain of colicin A. *Nature.* 354:408–410.
5. Parker, M. W., F. Pattus, …, D. Tsernoglou. 1989. Structure of the membrane-pore-forming fragment of colicin A. *Nature.* 337:93–96.
6. Parker, M. W., J. P. Postma, …, D. Tsernoglou. 1992. Refined structure of the pore-forming domain of colicin A at 2.4 A resolution. *J. Mol. Biol.* 224:639–657.
7. Lakey, J. H., D. Duché, …, F. Pattus. 1993. Fluorescence energy transfer distance measurements. The hydrophobic helical hairpin of colicin A in the membrane bound state. *J. Mol. Biol.* 230:1055–1067.
8. Massotte, D., M. Yamamoto, …, F. Pattus. 1993. Structure of the membrane-bound form of the pore-forming domain of colicin A: a partial proteolysis and mass spectrometry study. *Biochemistry.* 32:13787–13794.
9. Duché, D., J. Izard, …, D. Baty. 1996. Membrane topology of the colicin A pore-forming domain analyzed by disulfide bond engineering. *J. Biol. Chem.* 271:15401–15406.
10. Padmavathi, P. V., and H. J. Steinhoff. 2008. Conformation of the closed channel state of colicin A in proteoliposomes: an umbrella model. *J. Mol. Biol.* 378:204–214.
11. Ho, D., M. R. Lugo, …, A. R. Merrill. 2011. Membrane topology of the colicin E1 channel using genetically encoded fluorescence. *Biochemistry.* 50:4830–4842.
12. Kim, Y., K. Valentine, …, W. A. Cramer. 1998. Solid-state NMR studies of the membrane-bound closed state of the colicin E1 channel domain in lipid bilayers. *Protein Sci.* 7:342–348.
13. Zakharov, S. D., M. Lindeberg, …, W. A. Cramer. 1998. Membrane-bound state of the colicin E1 channel domain as an extended two-dimensional helical array. *Proc. Natl. Acad. Sci. USA.* 95:4282–4287.
14. Huang, C. H., and J. P. Charlton. 1972. Interactions of phosphatidylcholine vesicles with 2-p-toluidinylnaphthalene-6-sulfonate. *Biochemistry.* 11:735–740.
15. Wiener, M. C., and S. H. White. 1992. Structure of a fluid dioleoylphosphatidylcholine bilayer determined by joint refinement of x-ray and neutron diffraction data. III. Complete structure. *Biophys. J.* 61:434–447.
16. Wimley, W. C., and S. H. White. 1993. Membrane partitioning: distinguishing bilayer effects from the hydrophobic effect. *Biochemistry.* 32:6307–6312.
17. Seelig, J., and P. Ganz. 1991. Nonclassical hydrophobic effect in membrane binding equilibria. *Biochemistry.* 30:9354–9359.
18. Mayer, L. D., M. J. Hope, and P. R. Cullis. 1986. Vesicles of variable sizes produced by a rapid extrusion procedure. *Biochim. Biophys. Acta.* 858:161–168.
19. Chen, Y. H., and J. T. Yang. 1971. A new approach to the calculation of secondary structures of globular proteins by optical rotatory dispersion and circular dichroism. *Biochem. Biophys. Res. Commun.* 44:1285–1291.
20. Arias-Moreno, X., S. Cuesta-Lopez, …, A. Velazquez-Campoy. 2010. Thermodynamics of protein-cation interaction: Ca(+2) and Mg(+2)

binding to the fifth binding module of the LDL receptor. *Proteins.* 78:950–961.

21. Ptitsyn, O. B. 1995. How the molten globule became. *Trends Biochem. Sci.* 20:376–379.
22. Ptitsyn, O. B. 1995. Molten globule and protein folding. *Adv. Protein Chem.* 47:83–229.
23. Chan, H. S., M. R. Wattenbarger, …, K. A. Dill. 1991. Enhanced structure in polymers at interphases. *J. Chem. Phys.* 94:6–21.
24. Wattenbarger, M. R., H. S. Chan, …, K. A. Dill. 1991. Surface-induced enhancement of internal structure in polymers and proteins. *J. Chem. Phys.* 93:8343–8351.
25. Fieber, W., M. L. Schneider, …, K. Bister. 2001. Structure, function, and dynamics of the dimerization and DNA-binding domain of oncogenic transcription factor v-Myc. *J. Mol. Biol.* 307:1395–1410.
26. Lavigne, P., L. H. Kondejewski, …, C. M. Kay. 1995. Preferential heterodimeric parallel coiled-coil formation by synthetic Max and c-Myc leucine zippers: a description of putative electrostatic interactions responsible for the specificity of heterodimerization. *J. Mol. Biol.* 254:505–520.
27. Muhle-Goll, C., T. Gibson, …, A. Pastore. 1994. The dimerization stability of the HLH-LZ transcription protein family is modulated by the leucine zippers: a CD and NMR study of TFEB and c-Myc. *Biochemistry.* 33:11296–11306.
28. Muhle-Goll, C., M. Nilges, and A. Pastore. 1995. The leucine zippers of the HLH-LZ proteins Max and c-Myc preferentially form heterodimers. *Biochemistry.* 34:13554–13564.
29. Zhou, N. E., C. M. Kay, and R. S. Hodges. 1994. The role of interhelical ionic interactions in controlling protein folding and stability. De novo designed synthetic two-stranded alpha-helical coiled-coils. *J. Mol. Biol.* 237:500–512.
30. Litman, B. J. 1972. Effect of light scattering on the circular dichroism of biological membranes. *Biochemistry.* 11:3243–3247.
31. Nozaki, Y., B. K. Chamberlain, …, C. Tanford. 1976. Evidence for a major conformational change of coat protein in assembly of fl bacteriophage. *Nature.* 259:335–337.
32. Park, K., A. Perczel, and G. D. Fasman. 1992. Differentiation between transmembrane helices and peripheral helices by the deconvolution of circular dichroism spectra of membrane proteins. *Protein Sci.* 1:1032–1049.
33. Lakey, J. H., D. Massotte, …, F. Pattus. 1991. Membrane insertion of the pore-forming domain of colicin A. A spectroscopic study. *Eur. J. Biochem.* 196:599–607.
34. Dutta, K., A. Alexandrov, …, S. M. Pascal. 2001. pH-induced folding of an apoptotic coiled coil. *Protein Sci.* 10:2531–2540.
35. Bowie, J. U. 2005. Solving the membrane protein folding problem. *Nature.* 438:581–589.
36. Fiedler, S., J. Broecker, and S. Keller. 2010. Protein folding in membranes. *Cell. Mol. Life Sci.* 67:1779–1798.
37. White, S. H., and W. C. Wimley. 1999. Membrane protein folding and stability: physical principles. *Annu. Rev. Biophys. Biomol. Struct.* 28:319–365.
38. Leavitt, S., and E. Freire. 2001. Direct measurement of protein binding energetics by isothermal titration calorimetry. *Curr. Opin. Struct. Biol.* 11:560–566.
39. Weber, P. C., and F. R. Salemme. 2003. Applications of calorimetric methods to drug discovery and the study of protein interactions. *Curr. Opin. Struct. Biol.* 13:115–121.
40. Wiseman, T., S. Williston, …, L. N. Lin. 1989. Rapid measurement of binding constants and heats of binding using a new titration calorimeter. *Anal. Biochem.* 179:131–137.
41. Breslauer, K. J., E. Freire, and M. Straume. 1992. Calorimetry: a tool for DNA and ligand-DNA studies. *Methods Enzymol.* 211:533–567.
42. Matos, C., J. L. Lima, …, M. Bastos. 2004. Interaction of antiinflammatory drugs with EPC liposomes: calorimetric study in a broad concentration range. *Biophys. J.* 86:946–954.
43. Li, H., A. D. Robertson, and J. H. Jensen. 2005. Very fast empirical prediction and rationalization of protein pKa values. *Proteins.* 61:704–721.
44. Matos, C., B. de Castro, …, S. Reis. 2004. Zeta-potential measurements as a tool to quantify the effect of charged drugs on the surface potential of egg phosphatidylcholine liposomes. *Langmuir.* 20:369–377.
45. Milhaud, J., J. M. Lancelin, …, A. Blume. 1996. Association of polyene antibiotics with sterol-free lipid membranes: I. Hydrophobic binding of filipin to dimyristoylphosphatidylcholine bilayers. *Biochim. Biophys. Acta.* 1278:223–232.
46. Wieprecht, T., O. Apostolov, …, J. Seelig. 1999. Thermodynamics of the alpha-helix-coil transition of amphipathic peptides in a membrane environment: implications for the peptide-membrane binding equilibrium. *J. Mol. Biol.* 294:785–794.
47. Wieprecht, T., M. Beyermann, and J. Seelig. 2002. Thermodynamics of the coil-alpha-helix transition of amphipathic peptides in a membrane environment: the role of vesicle curvature. *Biophys. Chem.* 96:191–201.
48. Liu, L. P., and C. M. Deber. 1998. Uncoupling hydrophobicity and helicity in transmembrane segments. Alpha-helical propensities of the amino acids in non-polar environments. *J. Biol. Chem.* 273:23645–23648.
49. Moll, T. S., and T. E. Thompson. 1994. Semisynthetic proteins: model systems for the study of the insertion of hydrophobic peptides into preformed lipid bilayers. *Biochemistry.* 33:15469–15482.
50. Ben-Tal, N., A. Ben-Shaul, …, B. Honig. 1996. Free-energy determinants of alpha-helix insertion into lipid bilayers. *Biophys. J.* 70:1803–1812.
51. Bao, X., Y. Chen, …, G. A. Altenberg. 2005. Membrane transport proteins with complete replacement of transmembrane helices with polyalanine sequences remain functional. *J. Biol. Chem.* 280:8647–8650.
52. Bechinger, B. 2001. Membrane insertion and orientation of polyalanine peptides: a (15)N solid-state NMR spectroscopy investigation. *Biophys. J.* 81:2251–2256.
53. Zhang, Y. P., R. N. Lewis, …, R. N. McElhaney. 2001. Peptide models of the helical hydrophobic transmembrane segments of membrane proteins: interactions of acetyl-K2-(LA)12-K2-amide with phosphatidylethanolamine bilayer membranes. *Biochemistry.* 40:474–482.
54. Murphy, K. P., D. Xie, …, E. Freire. 1993. Structural energetics of peptide recognition: angiotensin II/antibody binding. *Proteins.* 15:113–120.
55. Tanford, C. 1980. The Hydrophobic Effect: Formation of Micelles and Biological Membranes. Chichester, New York.
56. Gonçalves, E., E. Kitas, and J. Seelig. 2005. Binding of oligoarginine to membrane lipids and heparan sulfate: structural and thermodynamic characterization of a cell-penetrating peptide. *Biochemistry.* 44:2692–2702.
57. Schwieger, C., and A. Blume. 2009. Interaction of poly(L-arginine) with negatively charged DPPG membranes: calorimetric and monolayer studies. *Biomacromolecules.* 10:2152–2161.
58. Kyte, J., and R. F. Doolittle. 1982. A simple method for displaying the hydropathic character of a protein. *J. Mol. Biol.* 157:105–132.
59. Sigurskjold, B. W. 2000. Exact analysis of competition ligand binding by displacement isothermal titration calorimetry. *Anal. Biochem.* 277:260–266.
60. Cho, W., and R. V. Stahelin. 2005. Membrane-protein interactions in cell signaling and membrane trafficking. *Annu. Rev. Biophys. Biomol. Struct.* 34:119–151.
61. Hurley, J. H., and T. Meyer. 2001. Subcellular targeting by membrane lipids. *Curr. Opin. Cell Biol.* 13:146–152.
62. Goñi, F. M. 2002. Non-permanent proteins in membranes: when proteins come as visitors (Review). *Mol. Membr. Biol.* 19:237–245 (Review).

63. Johnson, J. E., and R. B. Cornell. 1999. Amphitropic proteins: regulation by reversible membrane interactions (review). *Mol. Membr. Biol.* 16:217–235 (review).

64. Cornell, R. B., and S. G. Taneva. 2006. Amphipathic helices as mediators of the membrane interaction of amphitropic proteins, and as modulators of bilayer physical properties. *Curr. Protein Pept. Sci.* 7:539–552.

65. Seelig, J. 2004. Thermodynamics of lipid-peptide interactions. *Biochim. Biophys. Acta.* 1666:40–50.

66. Wieprecht, T., M. Dathe, …, M. Bienert. 1996. Conformational and functional study of magainin 2 in model membrane environments using the new approach of systematic double-D-amino acid replacement. *Biochemistry.* 35:10844–10853.

67. Wenk, M. R., and J. Seelig. 1998. Magainin 2 amide interaction with lipid membranes: calorimetric detection of peptide binding and pore formation. *Biochemistry.* 37:3909–3916.

68. Mosior, M., and S. McLaughlin. 1992. Binding of basic peptides to acidic lipids in membranes: effects of inserting alanine(s) between the basic residues. *Biochemistry.* 31:1767–1773.

69. Arnulphi, C., L. Jin, …, A. Jonas. 2004. Enthalpy-driven apolipoprotein A-I and lipid bilayer interaction indicating protein penetration upon lipid binding. *Biochemistry.* 43:12258–12264.